ELSEVIER

Journal of Alloys and Compounds 229 (1995) 107–122

Journal of ALLOYS AND COMPOUNDS

On the crystal chemistry of oxomercurates(II)

Hk. Müller-Buschbaum

Institut für Anorganische Chemie der Universität, Olshausenstr. 40–60, D-24118 Kiel, Germany

Received 6 December 1994; in final form 7 March 1995

Abstract

Recent results in the field of oxomercurate(II) chemistry are reviewed. The methods of preparation and the crystal chemistry of oxomercurates are discussed. The structures of the alkali metal oxomercurates (M_2HgO_4), alkaline earth oxomercurates ($MHgO_4$, $CdHgO_4$), rare earth oxomercurates, ternary oxomercurates ($BaAg_2Hg_2O_4$ and $Ba_3Pt_4HgO_{11}$) and the compounds $Ba_2Hg_2Pd_7O_{14}$, $HgCr_6$, $Hg_2Nb_2O_7$ and HgV_2O_6 are presented and analysed. The change in crystal chemical behaviour from oxomercurates to mercury-oxometallates is discussed.

Keywords: Crystal chemistry; Oxomercurates

1. Introduction

Only a few of the metallic elements reveal cationic as well as anionic features in the crystal chemistry of oxides. Of these elements, first and foremost are copper, silver and mercury. Because of the large number of copper compounds investigated, these two aspects of crystal chemistry should be explained with regard to the copper oxides. Two review articles [1,2] have reported that the predominant chemical role of the Cu^+, Cu^{2+} and Cu^{3+} ions in oxides formed by metallic elements (oxometallates) depends, in particular, on their chemical position in the network of the solids. The oxocuprates(I) show Cu^+ in a dumb-bell-like environment, whereas oxocuprates(II/III) show Cu^{2+} or Cu^{3+} in mainly square planar coordination formed by oxygen. The various copper ions form the anionic part of the crystal structure conjointly with oxygen ions in compounds called oxocuprates. However, if there are clearly perceptible polyhedra around the copper ions with higher coordination numbers, represented, for example, by capped or simple trigonal prisms, octahedra, trigonal bipyramids or polyhedra with irregular shapes, the crystal chemical function of the copper ions can be categorized as cationic, comparable with other metal ions in typical salts containing complex anionic groups of non-metallic elements. These compounds should be distinguished from the first group of oxocuprates by the expression copper-oxometallates. It has been shown in Ref. [2] that there is a gradual transition from the first to the second defined group rather than a gap between oxocuprates and copper-oxometallates.

The crystal chemistry of mercury-containing oxides has been investigated extensively over the last few years. This contribution shows that the crystal chemistry of mercury has characteristics which are visibly analogous to those indicated for the copper compounds. It is shown that mercury-containing oxides can be classified by the terms oxomercurates and mercury-oxometallates. Furthermore, it is shown that, between these two types of mercury-containing compound, a gradual change takes place in the crystal chemical behaviour of mercury.

Because of the difficulties in preparing mercury oxides and, in particular, their single crystals, the essential preparation methods used so far are discussed first.

As a result of the promising situation in the field of copper-containing high T_c superconducting oxides, it has been reported that mercury-containing oxides may create a new class of non-metallic superconductor. As

SSDI 0925-8388(95)01675-9

shown here, they belong to the group of oxomercurates(II).

2. Preparation techniques

2.1. Preparation under low oxygen pressure up to 100 bar

Due to the relatively low thermal stability and high volatility of mercury oxide, it is necessary to work in closed systems. A related problem of these techniques is the corrosive influence of oxygen on the autoclave materials with increasing temperature and pressure. Many of the mercury oxides were prepared in closed quartz glass ampoules under low oxygen pressure. The pressure which can be achieved in this manner is limited by the mechanical stability of the quartz tubes. It may be improved by taking into consideration the fact that quartz ampoules are capable of withstanding high external pressure. The explosion of quartz glass ampoules can easily be eliminated by ensuring that the external pressure is always greater than the internal pressure. This was performed by Rau and Rabenau [3,5] who introduced a new solvothermal method, using hydrochloric, hydrobromic or hydroiodic acid, which involved heating the quartz ampoules inside steel autoclaves initially filled with solid CO_2. In this way, the external pressure of evaporated CO_2 was higher than the pressure inside the quartz glass tubes. The limits of this method lie in the strong reactivity of quartz glass with gaseous basic oxides. SiO_2 glass either loses its mechanical stability by recrystallization or is changed to silicates beginning on the inside wall of the ampoules.

2.2. Preparation under oxygen pressures up to 1500 bar using CO_2 laser technique

Systems under high-pressure gaseous conditions have already been described elsewhere [4,5]. All suffer from the fact that the steel vessels are completely heated to higher temperatures and the autoclaves themselves react with the internal high-pressure oxygen atmosphere. A decade ago, we introduced a CO_2 laser technique [6] in solid state chemistry. This special application depends on high pressure for the preparation of new compounds using oxides that are more or less thermally unstable [7]. Fig. 1 shows an autoclave with a CO_2 laser-permeable window. The KCl window is sealed by ductile silver and indium rings. Before starting the heating process, the autoclave is filled with a pellet of the oxide mixture and with oxygen at the pressure of 150 bar of a connected

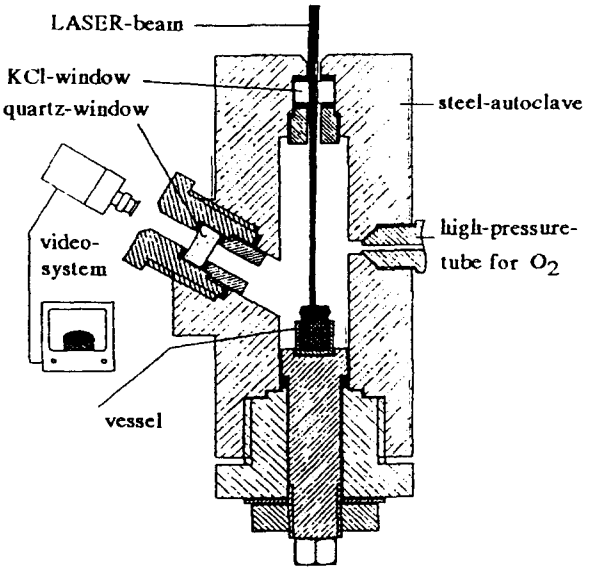

Fig. 1. Cross-section of the laser autoclave.

O_2 bomb. The silver and indium sealing rings, which are pressed towards the autoclave wall, become more and more dense with increasing pressure. Higher O_2 pressures (up to 2000 bar) can be achieved using a membrane compressor.

The irradiated energy of the focused laser beam is absorbed by most solid materials and changed into thermal energy within a small layer on the top of the pellet. The autoclave and the laser-permeable window, as well as the observation windows, remain stable against the aggressive oxygen atmosphere at the low temperature. The greatest limitation of this method is the small stability of the KCl laser window. It is invariably attacked spontaneously by the high-energy laser beam and destroyed by heating due to a thin film of evaporated material condensed on the window. This takes place, for example, when mercury oxide and a strongly focused laser beam with a high energy density are used on the surface of reacting pellets. Another limitation lies in the resulting deformation of the KCl window above 1500 bar oxygen pressure. KCl becomes flexible and the planar polished window surfaces are bent. As a result of this, the laser beam is scattered and the power supplied to the surface of the pellet is strongly diminished.

From these experiments, it was concluded that it is necessary to increase the oxygen pressure greatly with increasing temperature in order to prepare single crystals of mercury-containing oxides. Later, it was found that the growth of single crystals of ternary mercury oxides depends on the ability of supercritical oxygen to act both as a reactant and a solvent.

2.3. Preparation under oxygen pressures up to 6500 bar

A convenient method for high-pressure experiments using supercritical oxygen was introduced [8] for the synthesis of oxoargentates(I) with the composition $SrAg_6O_4$ [9] and $BaAg_6O_4$ [10]. This autoclave technique was recently extended to oxomercurates. In brief, an oxygen-resistant autoclave made of ATS steel is filled with the reacting oxide mixture and liquid oxygen and heated to 500–700°C. This procedure results in an internal oxygen pressure of the order of 6000 bar.

In order to handle these extreme conditions, a knowledge of the physical data of pure oxygen under pressure is required. The density of liquid oxygen as a function of temperature was reported in Refs. [11–14]. Fig. 2 shows the isothermic densities of gaseous oxygen [15,16] calculated with increasing pressure. It can be seen that, under high-pressure conditions, the density is of the order of that of liquid oxygen (1.218 g cm^{-3} [17]). Assuming there is no dead volume either within the liquid oxygen-filled autoclave or in the connected capillary system and the outlet valve, an estimated pressure of 4300 bar [8] at room temperature is obtained. The lower experimental value of 3000 bar is based on small unavoidable dead volumes during the filling of the autoclave with liquid oxygen.

The oxygen-filled autoclave should be heated up rapidly to 150°C and then slowly to the upper limit of 700°C. The internal pressure rises spontaneously and prevents the continuous loss of oxygen by leakage of the seals at the beginning of the heating process.

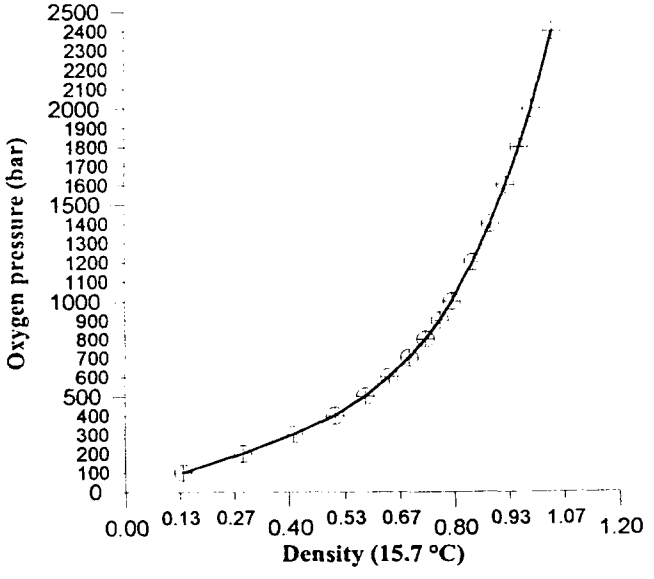

Fig. 2. Calculated isothermic density of liquid oxygen vs. pressure.

Temperatures higher than 700°C destroy the valuable steel autoclaves by reaction with the internal oxygen. All the damage observed starts at the point of the highly deformed Bridgeman seal and/or the thread under tension.

3. The crystal chemistry of oxomercurates(II)

3.1. General remarks

Compounds containing mercury can be roughly classified into salt-like oxides and oxomercurates. In the first group, mercury acts as a cation in typical non-metallic ionic salts. From the viewpoint of crystal chemistry, mercury ions are the opposite of more or less complex anionic groups. In the oxomercurates, which are discussed here, mercury and oxygen can both be seen as components of the anionic part of the crystal structure. Considering this aspect of crystal chemistry, this contribution focuses mostly on compounds in the oxomercurates category.

3.2. Oxomercurates with isolated O–Hg–O dumbbells

3.2.1. Superconductor-related oxomercurates(II) ($HgBa_2LnCu_2O_{7-x}$) and superconducting phases of the composition $HgBa_2Ca_{n-1}Cu_nO_{2n+2+x}$

The enthusiasm for the research of high-temperature superconducting oxides has recently led to mercury-containing compounds of the composition $HgBa_2LnCu_2O_{7-x}$ (Ln ≡ La, Nd, Eu, Gd, Dy, Y) [18] showing no superconductivity and superconducting phases of the composition $HgBa_2Ca_{n-1}Cu_nO_{2n+2+x}$ with $n = 1$ [19,20], $n = 2$ [21,22], $n = 3$ [23–25] and $n < 3$ [26,27]. The last two contributions quoted summarize the research in the field of mercury superconductors up to the present time. It should be mentioned that, under high-pressure conditions, the T_c value rises by approximately 1 K per gigapascal. The highest known T_c value is of the order of 150 K [25].

The crystal structure of $HgBa_2LnCu_2O_{7-x}$ strongly resembles the well-known Tl-1212 ($TlBa_2CaCu_2O_7$) superconductor, but shows mercury within a strictly linear oxygen coordination as can be seen in Fig. 3(a). The closest O^{2-} neighbours along the c axes of the tetragonal crystal structure show distances to mercury of 2.20 Å. The next adjoining oxygen sphere of the positions $x,y,z = 1/2,1/2,0$ enlarges the polyhedron to an octahedron of the type 4L + 2S (four long, two short) by distances of the order of 2.75 Å. In addition, Fig. 3(b) shows the spectacular mercury/copper superconductor $HgBa_2CuO_{4+x}$ [19]. The most significant

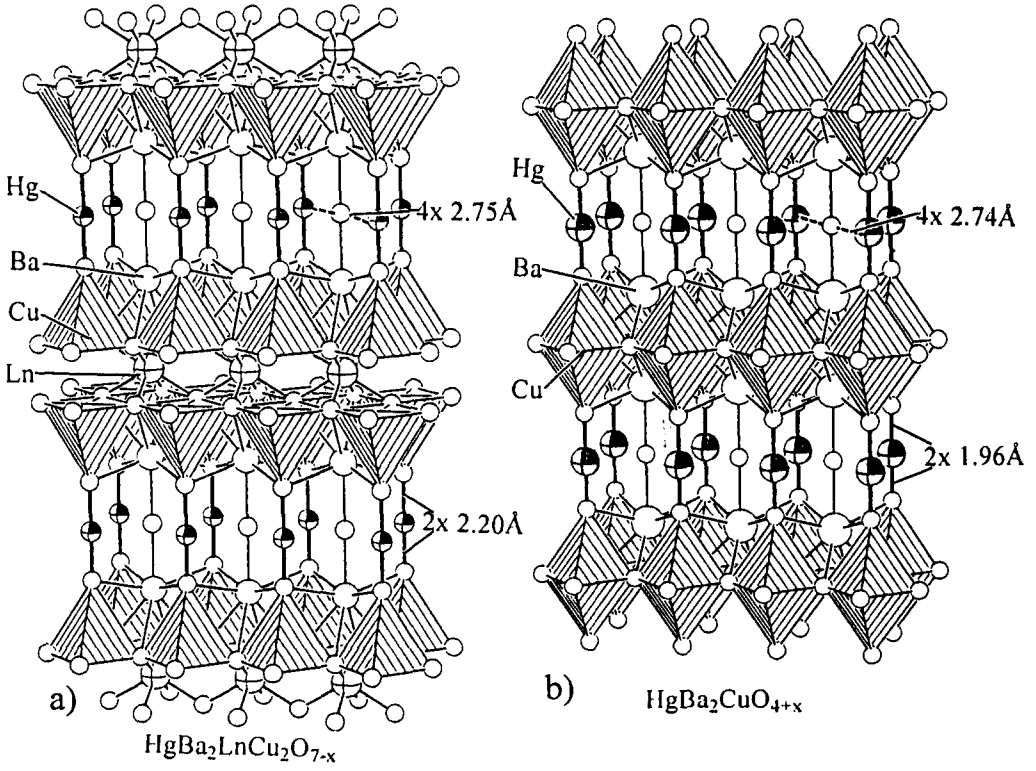

Fig. 3. Perspective views of the crystal structures of (a) $HgBa_2LnCu_2O_{7-x}$ (square pyramids around copper, hatched; spheres with black segment, Hg^{2+}; large open spheres, Ba^{2+}; large spheres with a cross, rare earth; the Hg–O bonds are emphasized) and (b) $HgBa_2CuO_{4+x}$ (CuO_6 octahedra, hatched; other symbols as in (a)).

differences with respect to $HgBa_2LnCu_2O_{7-x}$ are as follows: firstly, only one copper layer is obviously responsible for the superconductivity and, secondly, the coordination of mercury is practically reduced to a stretched O–Hg–O dumb-bell because of the small occupancy factor (SOF) of O(3) (SOF = 0.1) in the position $x,y,z = 1/2,1/2,0$.

3.2.2. Oxomercurates(II) of the alkaline metals: M_2HgO_2 (M ≡ Li–Cs)

Alkaline oxomercurates with the composition M_2HgO_2 [28] (M ≡ Li–Cs) have been well known since 1964. These compounds were prepared by heating intense mixtures of HgO and the oxides of alkaline metals (MO_x; $0.5 \leq x \leq 2$) in closed glass or quartz tubes. The crystal structure was determined with reference to single crystals of Na_2HgO_2 and verified by powder and single crystal work of K_2HgO_2. The other compounds with M ≡ Li, Rb and Cs were identified by powder techniques. The Na_2HgO_2 type shows tetragonal symmetry. A typical feature of the crystal structure is the square pyramidal coordination of the alkaline metals by oxygen. Fig. 4 shows two-dimensional edge-shared MO_5 polyhedra, forming layers of O^{2-} in square planar arrangements. Every square is completed to form a pyramidal polyhedron by a fifth O^{2-} ion along the *c* axis. As can be seen from the

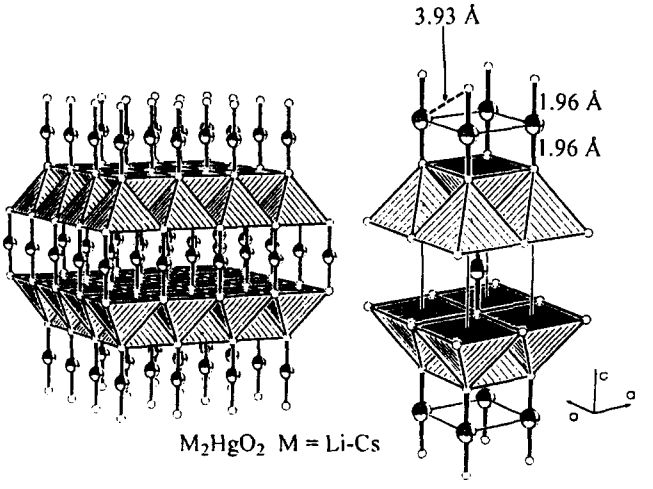

Fig. 4. Perspective view of the crystal structure of Li_2HgO_2–Cs_2HgO_2. The square pyramids of O^{2-} around Li^+–Cs^+ are hatched; large spheres with a black segment, Hg^{2+}; small spheres, O^{2-}; the Hg–O bonds are emphasized.

enlarged structure section of Fig. 4, there are also further square pyramids with an orientation of the apical oxygen in the [00 − 1] direction placed into the open area of the polyhedral arrangement discussed above. The polyhedral layers are staggered and connected along [001] by Hg^{2+} ions. The resulting coordination of Hg^{2+} can be described as a dumb-bell-like

O–Hg–O environment. The distances of the eight remote oxygen atoms (3.93 Å) of the second coordination sphere are so far away with respect to the shortest two (1.96 Å) that they cannot be counted as belonging to the resulting deformed coordination sphere.

It took more than 20 years to prepare single crystals of the alkaline earth mercury oxides first mentioned in 1969 [29] and to analyse the hitherto unknown crystal structures.

3.2.3. Oxomercurates(II) of the alkaline earth metals $BaHgO_2$, $Ba_{0.75}Sr_{0.25}HgO_2$ and $SrHgO_2$

Due to the relatively high reactivity of BaO (with respect to the other alkaline earth oxides), the ternary oxide $BaHgO_2$ [30] was the first example of the single crystal preparation of alkaline earth oxomercurates(II) under high oxygen pressure. Using dry oxygen ($BaHgO_2$ is extremely sensitive to traces of moisture), BaO and HgO, amber-coloured single crystals are formed within a reaction time of 5 days using 6000 bar oxygen pressure and a temperature of 700°C. X-Ray investigations led to an interesting crystal structure which can be explained step by step as shown in Fig. 5. It can be seen from Fig. 5(a) that the two barium positions Ba(1) and Ba(2) are coordinated sixfold by oxygen. The polyhedron can be described as strongly deformed trigonal prisms of different sizes and differently positioned Ba^{2+} ions. Ba(1) is placed in the centre of the oxygen polyhedron (6×2.59 Å), while Ba(2) obviously prefers an out-of-centre position (3×2.61 Å, 3×2.74 Å). The $Ba(2)O_6$ polyhedron is more distorted than the other polyhedron.

The $Ba(1)O_6$ prisms are connected by Hg^{2+} ions in the [001] direction, thus forming one-dimensional infinite chains as shown in Fig. 5(b). The other prism type, $Ba(2)O_6$, is partly connected in the same manner, resulting in groups of the sequence $O_3Ba(2)O_3$–$(Hg)_3$–$O_3Ba(2)O_3$, but without infinite connection straight along the c axis as demonstrated in Fig. 5(c). These significant differences in the connection of BaO_6 prisms and O–Hg–O dumb-bells are responsible for the in-centre and off-centre positioning of Ba^{2+} as described previously. The repulsive Coulomb action of the Hg^{2+} ions on Ba^{2+} works equally in both directions ($-z$ and $+z$) along the infinite chains. As a consequence of this, Ba^{2+} is fixed in the middle of the $Ba(1)O_6$ prisms. In addition, the interrupted chains of Fig. 5(c) show the divergent orientation of the peripheral O–Hg–O dumb-bells. The repulsive action of the three more distant peripheral Hg^{2+} ions on Ba^{2+} is weaker than that of the three centred Hg^{2+}. Consequently, Ba^{2+} is shifted to the outer prism plane. Finally, Fig. 5(d) shows layers of edge-shared BaO_6 prisms parallel to (110), whereas Fig. 5(e) demonstrates the torsion of the triangular prism planes relative to each other due to the corner connection by Hg^{2+} ions.

The difference in size of the $Ba(1)O_6$ and $Ba(2)O_6$ prisms gave rise to the idea of replacing Ba^{2+} partly by Sr^{2+}. Experiments in this direction led to a mixed compound of the composition $Ba_{0.75}Sr_{0.25}HgO_2$ [31]. The substituted quantity of Sr^{2+} is precisely correlated with the thorough replacement of Ba(2) by Sr^{2+} at the point position (2a). It results in the occupation of the bigger and stronger deformed trigonal prism by Ba^{2+} and the smaller one by Sr^{2+}.

A complete replacement of Ba^{2+} by Sr^{2+} or Ca^{2+} led to the compounds $SrHgO_2$ and $CaHgO_2$ [29]. Both were prepared and investigated using powder techniques [32] and the former was also independently investigated using single crystal techniques [33]. Due to the decreasing basicity in the row of oxides BaO, SrO and CaO, it has been impossible, so far, to prepare X-ray-relevant single crystals of $CaHgO_2$.

Yellowish single crystals of $SrHgO_2$ can be prepared by heating SrO and HgO for 6 days above 600–620°C using high oxygen pressures of 6000–6100 bar [33]. Analogous to the preparation of $BaHgO_2$, the equally moisture-sensitive crystals of $SrHgO_2$ should be placed in glass capillaries, together with a small piece of metallic sodium in order to collect X-ray data. Disregarding some differences in the symmetry determined, powder and single crystal investigations of $SrHgO_2$ [32,33] originally described this solid in accordance with the well-known Delafossite structure. A typical feature of this structure (Fig. 6(a)) is an edge sharing of SrO_6 octahedra in layers parallel to (110), which are connected along [001] by Hg^{2+} ions. After publication, a detailed look at the orientation of the $^2_\infty[SrO_2]$ planes relative to each other showed that $SrHgO_2$ is isotypic to the mineral Crednerite ($CuMnO_2$) [34].

Finally, Fig. 6(b) demonstrates the change from trigonal prismatic ($BaHgO_2$) to octahedral ($SrHgO_2$) coordination of the alkaline earth ions produced by increasing the torsion of the opposite triangular prism faces relative to each other.

It should be mentioned that a second form (obviously a low-pressure modification) of $BaHgO_2$ belonging to the Delafossite type has been discovered recently [35].

3.2.4. Oxomercurates of subgroup elements

3.2.4.1. Cadmium oxomercurate(II): $CdHgO_2$. High-pressure reactions of CdO and HgO have recently led to the formation of single crystals of the first cadmium oxomercurate(II) with the composition $CdHgO_2$ [36]. The original oxides react within 8 days at temperatures of the order of 600–620°C and 4200 bar oxygen pressure. Due to leakage of the autoclave, the pressure decreases to 3600 bar at the end of the reaction time. Orange-coloured single crystals, examined by X-ray

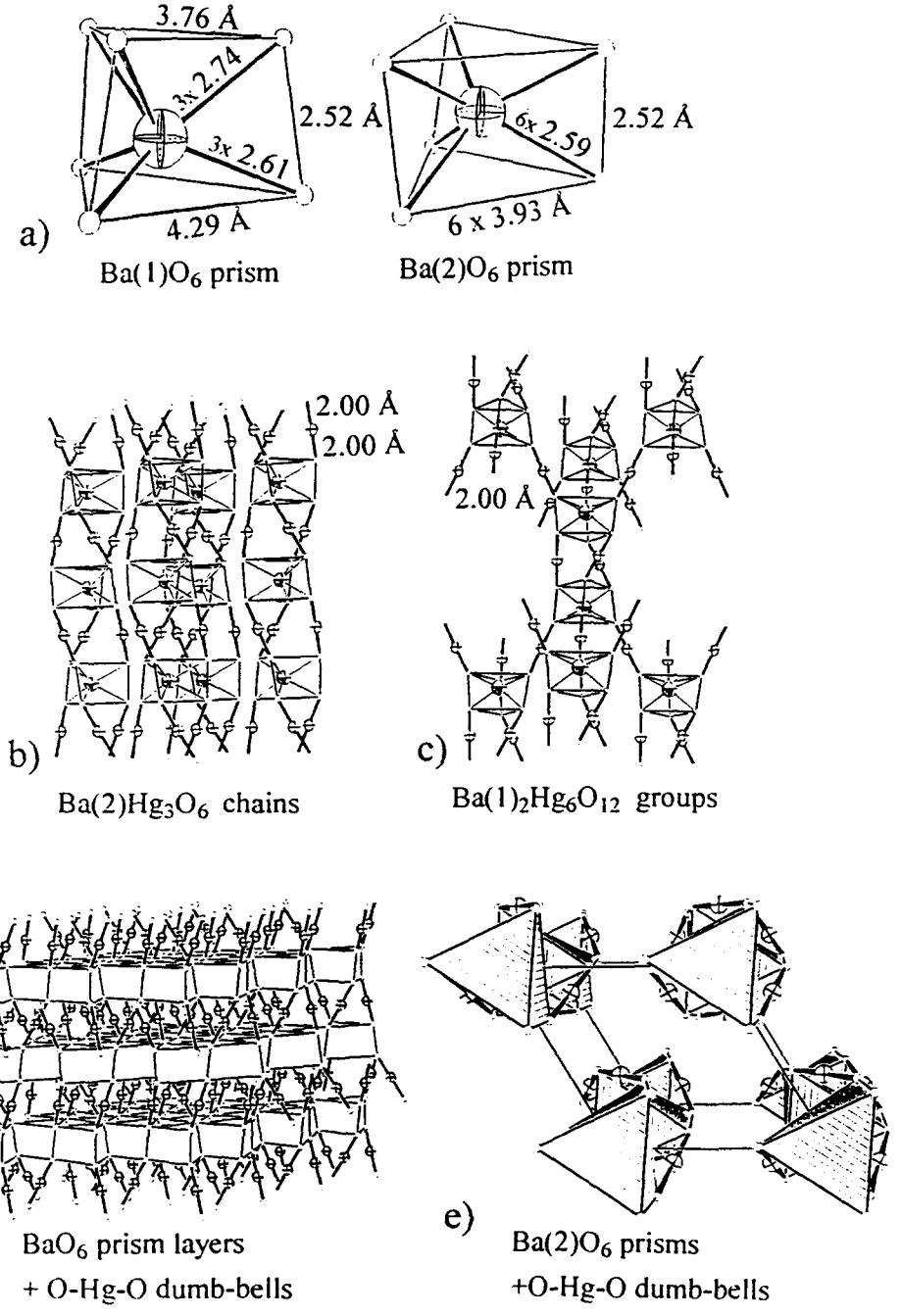

Fig. 5. Structural segments of $BaHgO_2$: (a) trigonal prismatic coordination of O^{2-} around Ba(1) and Ba(2); connection of $Ba(2)O_6$ (b) and $Ba(1)O_6$ (c) prisms by Hg^{2+} along [001]; (d) network of BaO_6 prisms parallel to (110) connected by Hg^{2+}; (e) torsion of trigonal BaO_6 prisms by obliquely connecting O–Hg–O dumb-bells.

methods, show a crystal structure closely related to the Crednerite type. Figs. 7(a) and 7(b) display the main differences from the above described compound $SrHgO_2$. The strictly orthogonal orientation to each other of the octahedral layers and O–Hg–O dumb-bells (Fig. 7(c)) in $SrHgO_2$ is altered by a parallel shift of the $^2_\infty[CdO_2]$ planes. This results in an angle between the linear O–Hg–O dumb-bells and the octahedral layers of the order of 59° (Fig. 7(d)). The idealized differentiation into 2S + 12L (1.96 Å and 4.3 Å) Hg–O distances in $SrHgO_2$ (undoubtedly coordination number two) shows a tendency towards a coordination number of six in $CdHgO_2$ exemplified by 2S + 4L (2.00 Å and 3.12 Å) Hg–O distances. The resulting polyhedron can be specified as a compressed octahedron of O^{2-} around Hg^{2+}. In the compound $CdHgO_2$, the characteristic dumb-bell-like coordination of Hg^{2+} ions in oxomercurates(II) (Hg^{2+} is part of the anionic

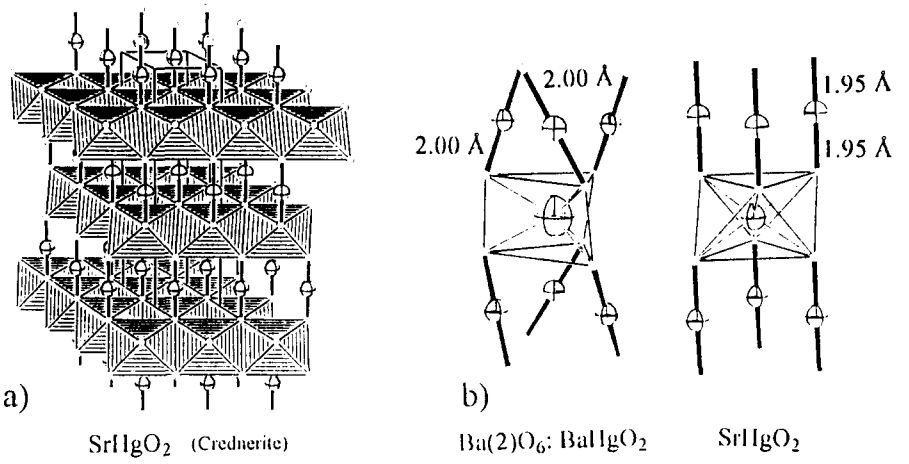

Fig. 6. (a) Perspective view of the crystal structure of $SrHgO_2$ (the in-plane edge-shared SrO_6 octahedra are hatched; large spheres with a cross, Hg^{2+}; small spheres, O^{2-}). (b) Orientation of O–Hg–O dumb-bells with respect to a trigonal BaO_6 prism ($BaHgO_2$) and an SrO_6 octahedron ($SrHgO_2$).

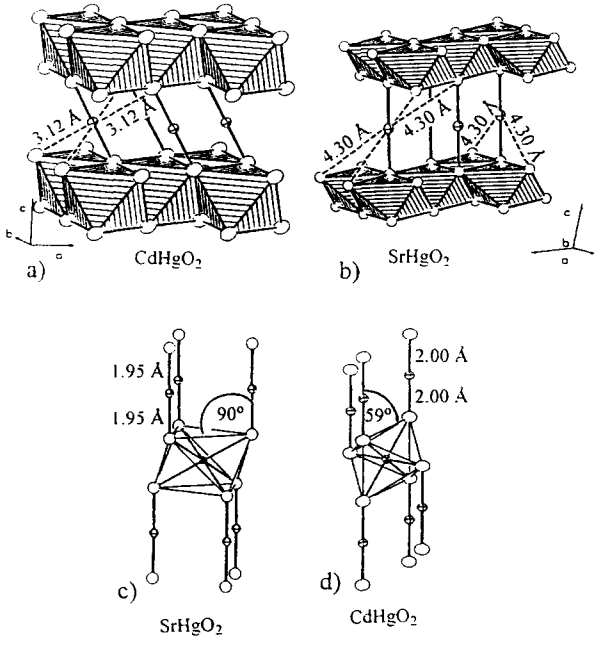

Fig. 7. Comparison of the orientation of CdO_6 and SrO_6 octahedral layers relative to each other in $CdHgO_2$ (a) and $SrHgO_2$ (b) and with respect to the O–Hg–O dumb-bells in $SrHgO_2$ (c) and $CdHgO_2$ (d) (spheres with crosses, Hg^{2+}; open spheres, O^{2-}).

component of the solids) shifts towards a more cationic behaviour of the Hg^{2+} ions which is discussed later.

It is of interest here to look at the crystal structures of $HgMoO_4$ and $HgWO_4$, prepared from $HgCl_2$ and Na_2MO_4 by heating to 700°C under a hydrostatic pressure of the order of 3000 bar. The isotypic compounds show octahedral layers very similar to $CdHgO_2$ connected by Hg^{2+} ions. Figs. 8(a) and 8(b) show two orientations of the O–Hg–O dumb-bells between the MoO_6 octahedral layers. The slanted orientation of O–Hg–O with respect to the octahedral layers gives four adjacent (2×2.67 Å, 2×2.77 Å) and two distant (3.14 Å) members in addition to the nearest oxygen neighbours (2×2.03 Å). With respect to the resulting polyhedron around mercury, the preceding discussion for $SrHgO_2$ and $CdHgO_2$ is also valid here. Finally, the reader's attention should be drawn to the unusual coordination number of six of molybdenum in oxides. The change from a mostly tetrahedral environment to an octahedral environment is due to the high-pressure preparation.

3.2.4.2. Oxomercurates with rare earth elements: Ln_2HgO_4 (Ln ≡ La, Nd, Sm, Eu, Gd, Ho). The history of the oxomercurates Ln_2HgO_4 shows the same duplication of discovery. They were prepared independently by low-pressure powder techniques [37] with the elements Ln ≡ La, Nd–Gd using closed quartz tubes and by high-pressure techniques for the synthesis of single crystals of Ho_2HgO_4 [38]. For the preparation of single crystals, it is necessary to maintain the oxygen pressure at 6200 bar and the temperature at above 620°C for over 1 week. The light yellowish single crystals are also sensitive to moisture. The crystal structure of this family is more complicated than the structures described so far. The structure is dominated by a network of trigonal prisms around the Ln^{3+} ions. Fig. 9(a) shows that the $Ho(1)O_6$ and $Ho(2)O_6$ prisms are monocapped by a seventh O^{2-} ion. The Ho^{3+} ions are positioned out of the prism centre, nearly in the plane of one of the rectangular prism faces. Fig. 9(b) shows details of the entire structure. There are chains of edge-connected trigonal prisms comparable with those of the Sr_2CuO_3 structure [39]. These $^1_\infty[Ho_2O_3]$ double prism chains are

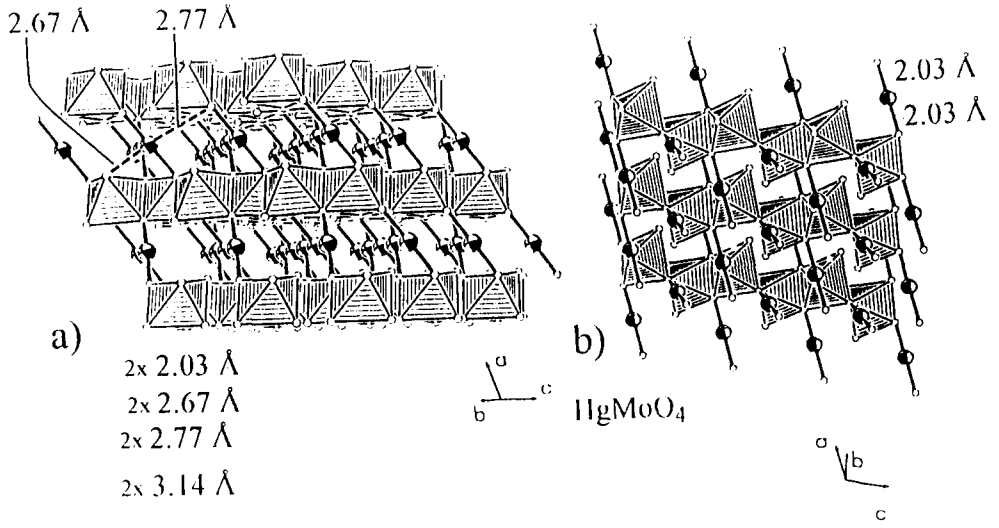

Fig. 8. Perspective drawing of MoO_6 octahedral layers (a) along [010] and (b) along [100] in the high-pressure oxide $HgMoO_4$ (large spheres with crosses, Hg^{2+}; small open spheres, O^{2-}; the Hg–O bonds are emphasized).

connected by the seventh capping O^{2-} neighbour forming infinite layers which at first seem isolated from each other. However, Fig. 9(c) completes the structural section of Fig. 9(b) to form a three-dimensional prism network. It shows that the prism layers displayed so far are connected by additional LnO_6 prisms in a complicated way. A sequence of two LnO_6 prisms is required to connect the neighbouring layers of Fig. 9(b) to each other. Finally, it can be seen in Fig. 9(c) that the Hg^{2+} ions (segmented spheres) are incorporated in the remaining small holes of this voluminous polyhedral network resulting in the characteristic O–Hg–O dumb-bell coordination of the oxomercurates(II) described above.

3.2.4.3. Barium–silver oxomercurate(II): $BaAg_2Hg_2O_4$. Ag^+ ions, as well as Hg^{2+} ions, are often coordinated by two oxygen ions in a dumb-bell-like arrangement as mentioned in Section 1. It was of great interest to prepare an oxide containing silver and mercury in order to investigate the crystal chemistry of both ions within the same solid. Under high-pressure conditions (6000 bar oxygen, 630°C), we prepared single crystals of $BaAg_2Hg_2O_4$ [40]. Fig. 10(a) shows that the crystal structure of this barium–silver–mercury oxide is characterized by layers of edge-connected BaO_8 cubes. This results in a planar net of filled and empty cubes. The Hg^{2+} ions are incorporated along the diagonals of the empty cubes, leading to the well-known O–Hg–O dumb-bell coordination. In order to achieve the usual bond distances between mercury and oxygen, the diagonals of the empty cubes are shortened. As a consequence, the BaO_8 cubes are distorted. The $^2_\infty[BaHg_2O_4]$ layers (see Fig. 10(b)) are stacked along [001] and connected by the Ag^+ ions. It should be mentioned that, in spite of the identical crystal chemical behaviour of Hg^{2+} and Ag^+, there is no exchange at the different crystal positions. The structural segment in Fig. 10(c) again shows the orientation and bond length of O–Ag–O and O–Hg–O dumb-bells with respect to the distorted BaO_8 cubes.

3.2.4.4. Barium oxoplatinate(II,V)-mercurate(II): $Ba_3HgPt_4O_{11}$. Despite the fact that this oxide may be classified as an oxoplatinate, it is discussed here from the viewpoint of mercury oxides showing mercury as a part of the anionic structural component. Single crystals of this mixed oxide were prepared from the intermetallic phase $PtHg_2$ and BaO reacting under high-pressure conditions [41]. During a reaction time of 8 days at 620°C, the original oxygen pressure of 4200 bar decreased to 3600 bar due to leakage of the Bridgeman seal. Finally, the synthesis resulted in black single crystals of good X-ray quality. The problems of solving the crystal structure with three heavy elements with almost the same X-ray scattering are described in Ref. [41].

Fig. 11(a) shows a polyhedral network of face-shared PtO_6 octahedra, square planar PtO_4 polygons and O–Hg–O dumb-bells. With respect to the Ru_2O_9 double octahedra shown in Fig. 11(b), there is a crystal chemical relationship between $Ba_3HgPt_4O_{11}$ and the precious metal 6L-perovskite $Ba_3CaRu_2O_9$ [42–45], as well as the tantalum perovskite $Ba_3SrTa_2O_9$ [46]. In these perovskites, the M_2O_9 double octahedra are connected by single MO_6 octahedra, which are formally replaced in $Ba_3HgPt_4O_{11}$ by square PtO_4 polygons

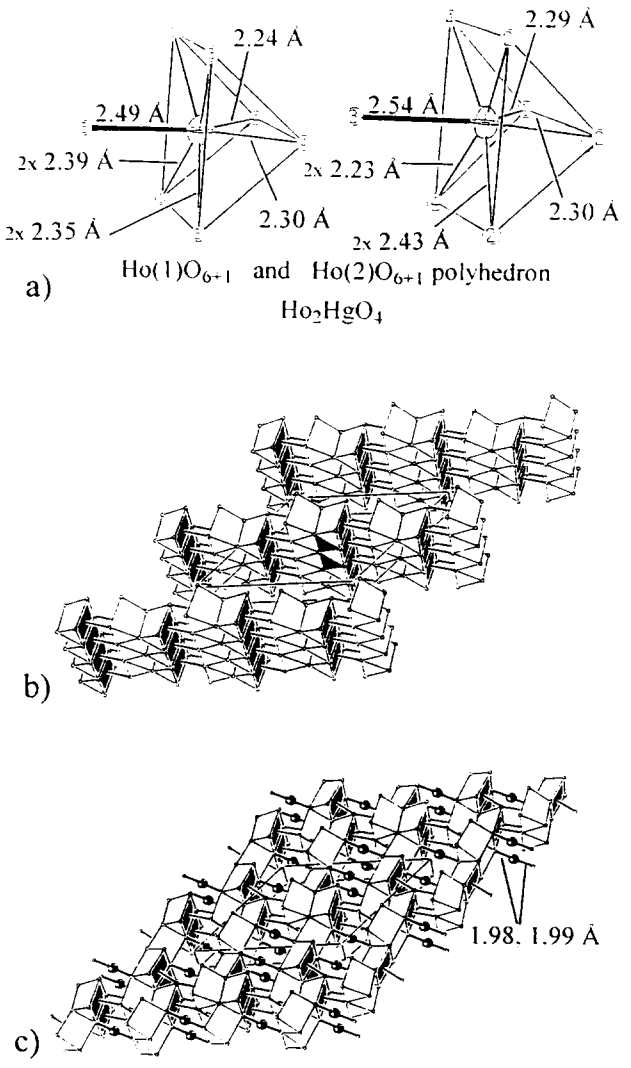

Fig. 9. (a) Single monocapped trigonal prisms of O^{2-} in Ho_2HgO_4 around Ho(1) and Ho(2). (b) Edge connection of trigonal HoO_6 prisms by double prisms forming cords and their two-dimensional connection by the seventh oxygen. (c) Three-dimensional network of trigonal HoO_6 prisms and O–Hg–O dumb-bells (large spheres with black segment, Hg^{2+}).

and O–Hg–O dumb-bells. The spaces inside the polyhedral network of Fig. 11(a) are filled by barium ions.

Ba(1) shows a cuboctahedral oxygen environment (Fig. 11(c)) with immediate contact to the faces of three Pt_2O_9 groups (Fig. 11(d)). It is interesting that the coordination sphere of Ba(2) is identical to that of Fig. 12(d) ($Ba_2Hg_3Pd_7O_{14}$). Figs. 11(e) and 11(f) reveal an infinite polyhedral chain of face- and edge-connected $Ba(2)O_{11}$ polyhedra. The face-shared $Ba(2)_2O_{19}$ double polyhedron of Fig. 11(e) is also connected by three Pt_2O_9 double octahedra. It is worth pointing out that $Ba_3HgPt_4O_{11}$ represents the rare oxidation state of Pt^{5+} in platinum oxides [41].

3.3. Oxomercurates(II) with linked O–Hg–O dumb-bells

3.3.1. Barium oxopalladate(II,IV)-mercurate(II): $Ba_2Hg_3Pd_7O_{14}$

In accordance with the definition of the barium–platinum–mercury oxide described above, the palladium-rich compound $Ba_2Hg_3Pd_7O_{14}$ may be ascribed to the palladium oxides as well as to the oxomercurates. It will be discussed here from the viewpoint of mercury oxides, showing mercury as part of the anionic structural component, as well as in terms of the crystal chemical role of salt-like mercury cations. The crystal structure can be described using single polyhedra, structural sections and the entire polyhedral network summarized in Fig. 12(f). Fig. 12(a) shows the octahedral environment of Pd^{4+} and Fig. 12(b) illustrates the expected square planar polygons around Pd^{2+}. In the latter figure, it can be seen that the two opposite edges of a central square planar PdO_4 polygon are bridged by two additional PdO_4 polygons. The resulting small triangles are, simultaneously, faces of PdO_6 octahedra within the crystal structure. The edge sharing of PdO_4 polygons in the enlarged structural section of Fig. 12(b) leads to $^2_\infty[PdO]$ layers as can be seen in Fig. 12(e). The total view of Fig. 12(f) demonstrates the above described linkage of $Pd^{4+}O_6$ octahedra with $Pd^{2+}O_4$ polygons and mercury ions. A specific detail of Fig. 12(f) involves the corner connection of two opposite PdO_6 octahedra (distinguished by the symbol Pd^{4+}) by square planar PdO_4 polygons along [001] at $z = 0.5$. Polygons of this square planar type in the middle of the c axis form one-dimensional zig-zag chains as is well known from the first high T_c superconductor $YBa_2Cu_3O_{6-x}$, for example. Fig. 12(f) also shows the linkage of opposite PdO_6 octahedra (symbol Pd^{4+}) by Hg^{2+} ions. This linkage results in adjacent oxygen ions firstly in a stretched O–Hg(1)–O coordination (spheres with a cross) and secondly in a so far unknown one-sided surrounding of Hg(2) by O(2) and O(5) (spheres with black segments in Fig. 12(f)). The six additional oxygen ions ($2 \times O(1)$ and $4 \times O(4)$) on the opposite sides of the coordination sphere of Fig. 12(c) show distinctly larger distances from mercury of the order of 2.79–3.29 Å. The resulting extended $Hg(2)O_{3+6}$ polyhedron can roughly be compared with the barium environment of Fig. 12(d). The great similarity of the Ba_2O_{20} group to parts of the Ba_2O_{17} chains (Fig. 11(f)) should be pointed out. The polyhedron around barium may be accepted as a damaged cuboctahedron with the loss of one oxygen ion. Two of them are connected in the outlined manner.

A look at Fig. 12(f) shows a connection of mercury–oxygen polygons which occurs in the mercury oxides

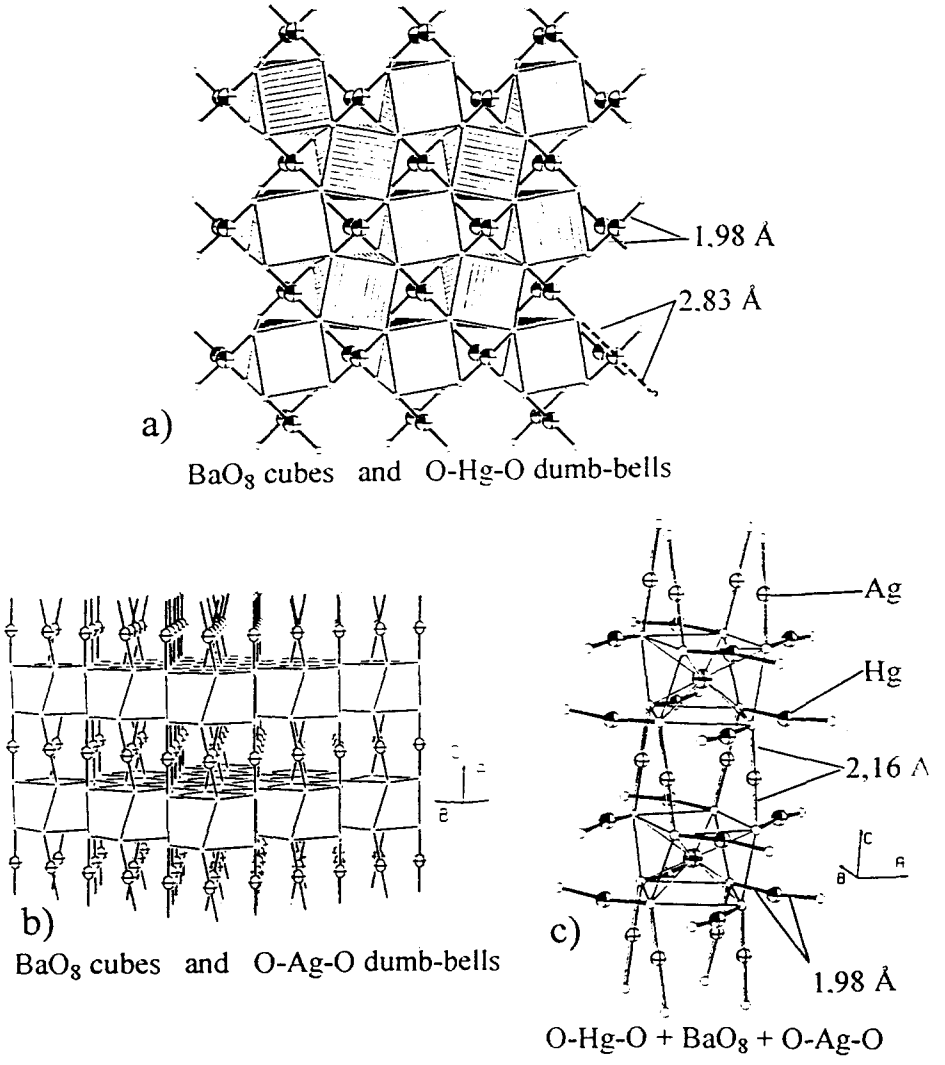

Fig. 10. (a) Projective drawing of one layer of BaO_8 cubes and in-plane O–Hg–O dumb-bells in $BaAg_2Hg_2O_4$. (b) Perspective drawing of stacked BaO_8 layers connected by Ag^+ ions. (c) Orientation of O–Hg–O and O–Ag–O dumb-bells with respect to the BaO_8 cubes (large spheres with black segment, Hg^{2+}; large spheres with crosses, Ba^{2+}; small spheres with crosses, Ag^+; small open spheres, O^{2-}).

described to date. In this case they form Hg_2O_6 groups isolated from each other. The claim made above that O–Hg–O dumb-bells are typical of oxomercurates(II) and that higher coordinated Hg^{2+} ions lean towards cationic behaviour implies here a direct connection of both properties in the Hg_2O_6 groups.

3.3.2. Nets of O–Hg–O dumb-bells. A mercury oxochromate(IV): $Hg_3O_2CrO_4$

High-pressure reactions led by chance to red single crystals of Hg_3CrO_6 [47]. Crystals of good quality have been prepared by heating a mixture of HgO and CrO_3 up to 600°C for more than 8 days. If we look at the chemical formula, it may seem that this compound belongs to the group of ordinary salts with Hg^{2+} cations and CrO_4^{2-} anions. Contrary to this impression, the crystal structure demonstrates a mixed oxide with shifts from the typical anionic group O–Hg–O (a feature of the oxomercurates(II)) to salt-like higher coordinated mercury. Fig. 13(a) indicates (in projection) two-dimensional nets of six-membered O–Hg–O rings, disregarding the distances longer than 2.2 Å. In reality these nets are somewhat twisted, as can be seen in the perspective drawing of Fig. 13(b). Each $(HgO)_6$ ring is filled by a CrO_4 tetrahedron. The large temperature factors of some oxygen positions, found during parameter refinement, were interpreted by split positions [47]. Thus there are evidently two "frozen" orientations of the CrO_4 tetrahedron expressed by the hatched and unshaded tetrahedra of Fig. 13(c).

The neighbourhood of the Hg(1) and Hg(2) positions merits further discussion. In addition to the short distances of 2.16–2.17 Å (Hg(1)–O) and 2.08 Å (Hg(2)–O), Figs. 13(d) and 13(e) show four more

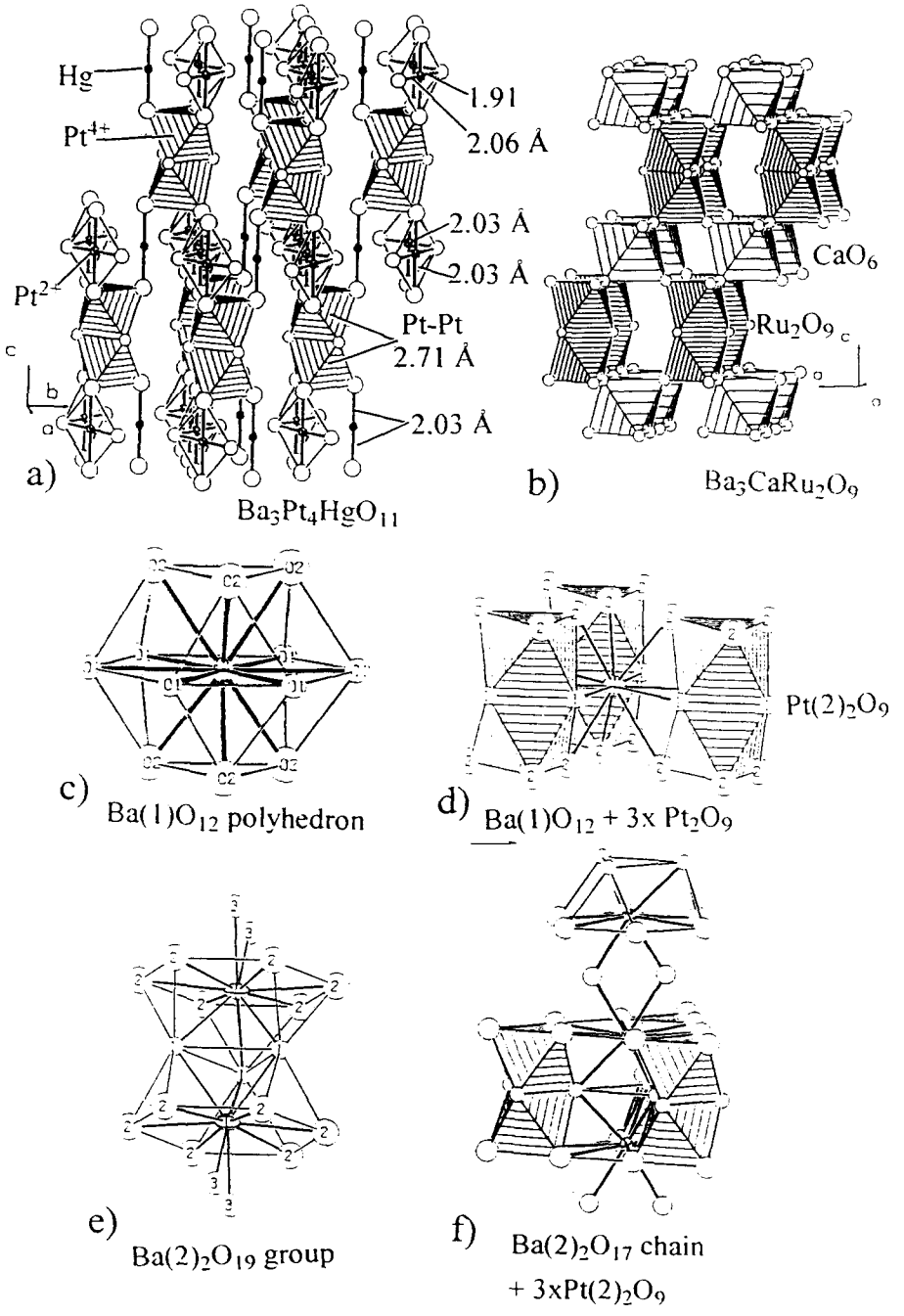

Fig. 11. Structural sections of $Ba_3Pt_4HgO_{11}$ (a, c–f) and comparison with $Ba_3CaRu_2O_9$ (b). (a) Perspective drawing of the connection of Pt_2O_9 double octahedra, square planar PtO_4 polygons and O–Hg–O dumb-bells. (c) Oxygen environment of Ba(1). (d) Linkage of the BaO_{12} polyhedron with three Pt_2O_9 groups. (e) Ba_2O_{19} group. (f) Connection of Ba_2O_{19} group with Pt_2O_9 double octahedra.

distant oxygen ions in the range 2.36–2.88 Å. The O–Hg(1)–O dumb-bell is completed to form a distorted octahedron (Fig. 13(d)) and O–Hg(2)–O achieves an irregular environment (Fig. 13(e)) by adding the more distant oxygen ions. When taken together, both the longer and shorter neighbours result in an HgO_6 polyhedron that is characteristic of cationic mercury in salts.

This viewpoint can also be applied to the crystal chemistry of mercury oxide. HgO exists in two modifications. The orthorhombic form [48–51] shows $^{1}_{\infty}$[HgO] zig-zag chains (Fig. 14(a)) situated in layers parallel to the *a*/*b* plane (Fig. 14(b)). The Hg–O distances are of the order of 2.02 Å. The hexagonal modification [52,53] is characterized by a coil of infinite–O–Hg–O–connections along the hexagonal *c*

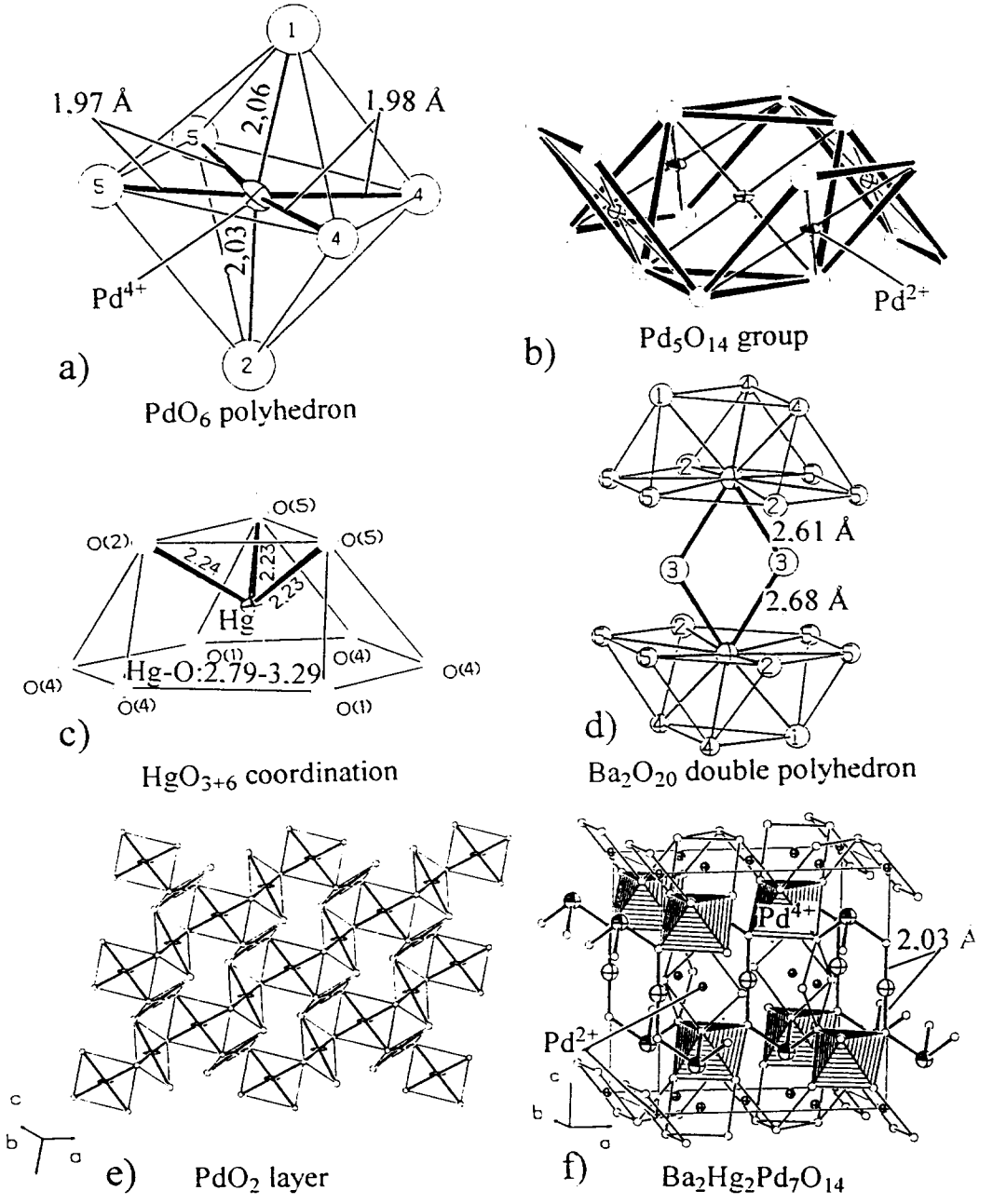

Fig. 12. Structural details of $Ba_2Hg_2Pd_7O_{14}$ (a–e) and the barium-free network (f). (a) $Pd^{4+}O_6$ octahedron. (b) Bridging of opposite edges of the square planar $Pd^{2+}O_4$ polygon by two additional planar PdO_4 groups. (c) Nearly one-sided open coordination of Hg(1). (d) Coordination sphere of barium and its connection to Ba_2O_{20} groups. (e) Layers made of corner-connected PdO_4 polygons. (f) Three-dimensional network of polygons around palladium and mercury.

axis (Fig. 14(c)). A look along [001] (Fig. 14(d)) shows what are almost triangular coils due to the small deviation of the O–Hg–O angles from 180°. There can be no doubt about the correlations in the third dimension, although the next sphere of oxygen neighbours is far away (2×2.8–2.9 Å, orthorhombic; 2×2.8–2.9 Å, hexagonal) in both modifications. The coordination number two is, however, ascribed to mercury in its pure oxides.

3.3.3. Framework of O–Hg–O dumb-bells: $Hg_2Nb_2O_7$, $Hg_2Ta_2O_7$ and $Hg_2Sb_2O_7$

As shown above, the O–Hg–O dumb-bells may be connected to each other forming groups and chains. All of these cases show oxygen surrounded by two Hg^{2+} ions. The next step towards two-dimensional nets and three-dimensional networks evokes a threefold oxygen coordination by mercury. This is observed for the compound $Hg_3O_2CrO_4$, the Pyro-

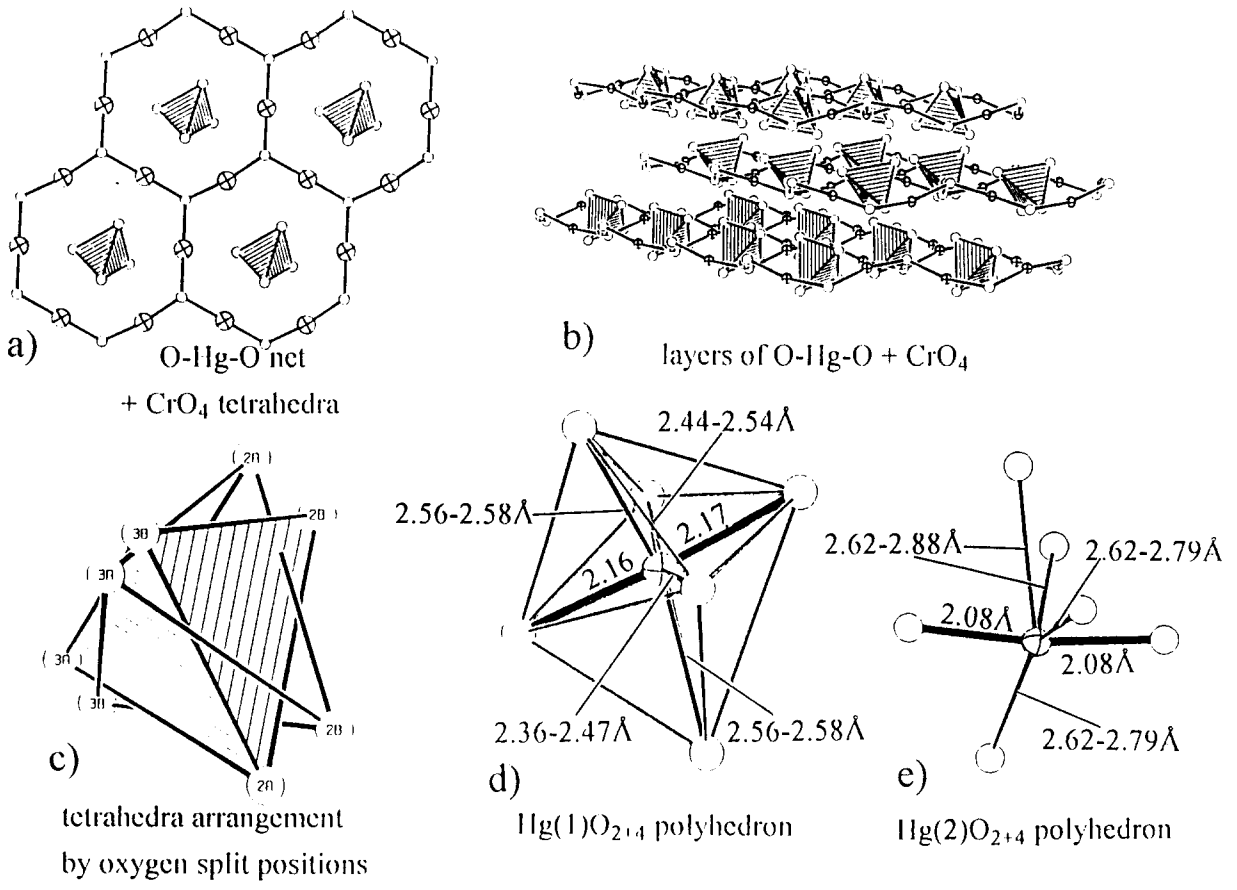

Fig. 13. Features of $HgCrO_6$. (a) Two-dimensional nets of O–Hg–O dumb-bells and incorporated CrO_4 tetrahedra. (b) Demonstration of twisting of the mercury–oxygen nets including the CrO_4 tetrahedra. (c) Separation of oxygen split positions into two tetrahedral orientations (d) and (e) O–Hg–O dumb-bells (emphasized bonds) completed by more distant oxygen neighbours.

chlor-related compound $Hg_2Nb_2O_7$ and its isotypic counterparts $Hg_2Ta_2O_7$ and $Hg_2Sb_2O_7$ [54]. Fig. 15(a) shows the three-dimensional network of linear O–Hg–O dumb-bells and Fig. 15(b) illustrates the superposition of NbO_6 octahedra in a Pyrochlor arrangement on the network of Fig. 15(a). Attention should be paid to the fact that the Hg–O distances fluctuate within a small range from 2×2.26 to 4×2.62 Å. We should be sceptical about the simplification of coordination number two and the classification of these compounds as oxomercurates(II) in general. $Hg_2M_2O_7$ (M ≡ Nb, Ta, Sb) may just as well be classified as salt-like mercury oxides (see below).

4. Salt-like mercury-containing oxometallates

4.1. Mercury oxovanadate: HgV_2O_6

At the end of this brief paper on the crystal chemistry of oxomercurates(II), one example is introduced of a mercury oxovanadate HgV_2O_6 [55] with mercury in a cationic function analogous to that seen for $Hg_2Nb_2O_7$. Fig. 16 exhibits three characteristic parts of the complete crystal structure. Fig. 16(a) shows fields of VO_n polyhedra in the unit cell area $x = 0.25$ and $x = 0.75$. The value of n depends on the distances between V^{5+} and O^{2-} (1.56, 1.62, 2.10, 2.25, 2.37, 2.56 and 2.74 Å) and cannot be defined exactly. The emphasized Hg^{2+} ions and O–Hg–O bonds connect the VO_n polyhedra along [100]. The inner sphere bond distance from mercury to oxygen is 2.03 Å, but it can be seen in Figs. 16(b) and 16(c) that an octahedral coordination of mercury is created by additional oxygen neighbours (2×2.42 and 2×2.47 Å). The differences between the distances of the compressed HgO_6 octahedra are of the order of those in $Hg_2Nb_2O_7$. This implies that a pure dumb-bell-like coordination is out of the question.

5. Conclusions

The classification postulated here into oxomercurates(II), containing more or less stretched O–Hg–O dumb-bells with the coordination number two typical

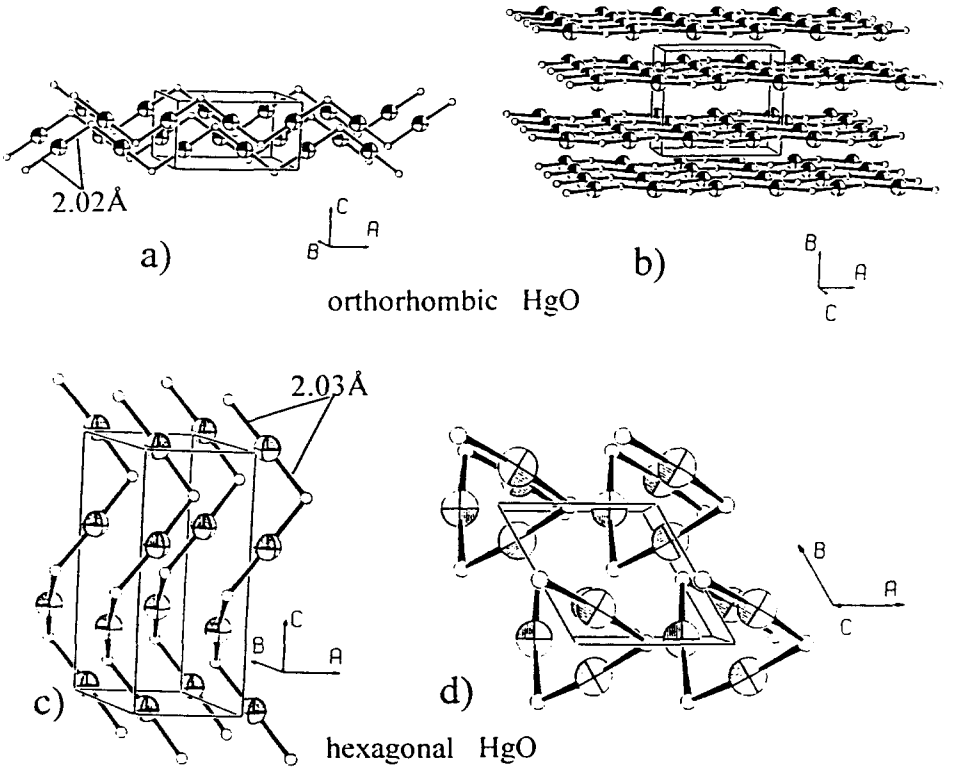

Fig. 14. Hg–O junction in mercury oxide: (a,b) orthorhombic; (c,d) hexagonal. Large sphere, Hg^{2+}; small open sphere, O^{2-}.

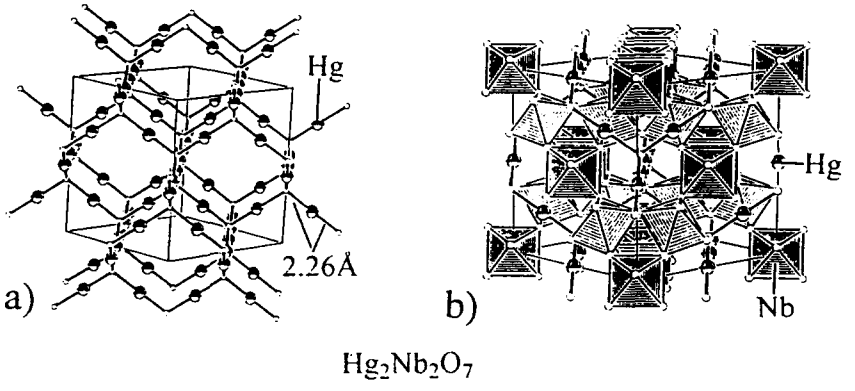

Fig. 15. (a) Idealized picture of the inner sphere environment of Hg^{2+} in $Hg_2Nb_2O_7$ neglecting more distant oxygen. (b) Combination of the NbO_6 octahedra and the O–Hg–O dumb-bells of (a).

of mercury, and mercury oxides, containing Hg^{2+} ions with a cationic crystal chemical function, arose from the crystal chemistry of oxocuprates [2] as mentioned in Section 1. It can be shown that the coordination spheres of Cu^{+} (O–Cu–O dumb-bells), Cu^{2+} (square planar coordination and square pyramids with copper nearly in the centre of the square face of these pyramids) and Cu^{3+} (square planar polygons) are typical features of copper in the anionic part of the crystal lattice. The chemistry of copper oxides is full of examples showing distinct steps from the oxocuprates to the copper oxometallates. The chemistry of mercury oxides described here also shows clearly perceptible shifts from the crystal chemistry of the oxomercurates to mercury oxometallates.

As can be seen from the alkaline and alkaline earth mercury oxides, compounds such as M_2HgO_2 (M ≡ Li–Cs) and $MHgO_2$ (M ≡ Ca–Ba) undoubtedly show a coordination number two of mercury in relation to oxygen. Both Hg^{2+} and O^{2-} are components of the anionic part of these solids. The same insight goes for compounds with large cations of high basicity represented by the rare earth elements (see Section 3.2.4.2). It is of great interest that the different ions Ag^{+} and

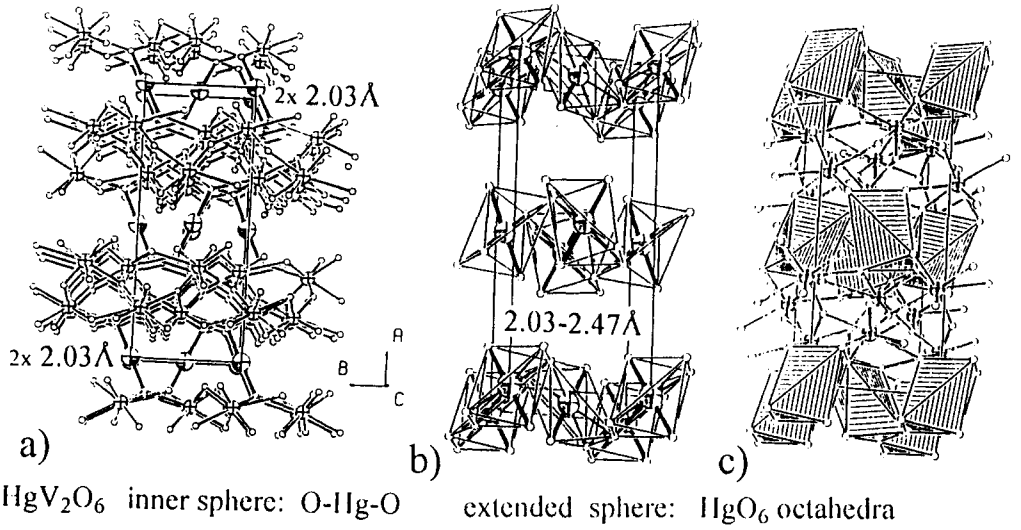

Fig. 16. (a) Idealized linear O–Hg–O environment (emphasized) in HgV_2O_6 connected to the vanadium–oxygen polyhedra. Polyhedra around mercury of the more distant oxygen neighbours in an open (b) and shaded (c) drawing.

Hg^{2+}, which both prefer dumb-bell-like coordination, act together on the doubtless cationic barium as parts of the anionic substructure. The large, but usually more covalently bonded, Cd^{2+} ion alters the chemical behaviour of mercury in a more cationic direction. This observation may be extended to compounds with small amounts of strongly basic ions, as demonstrated for $Ba_2Hg_3Pd_7O_{14}$. Both mercury and palladium take part in the anionic structure by forming O–Hg–O dumb-bells and square planar PdO_4 polygons. The strength of the individual tendencies of the Hg^{2+} and Pd^{2+} ions to stay in the anionic part of the structure is an open question in this context. The unusual one-sided open coordination of Hg^{2+} in $Ba_2Hg_3Pd_7O_{14}$ shows clearly that the loser in the competition to be part of the anionic lattice is one of the two mercury positions, namely Hg(2). A small, but obvious, shift from the pure anionic to the more cationic behaviour of Hg(2) is established by the HgO_{3+6} polyhedron in $Ba_2Hg_3Pd_7O_{14}$. The other examples given in this review show moderate changes from the coordination number of two to higher values, corresponding to shifts in the direction of cationic Hg^{2+} in the definition of oxomercurates(II).

It should be mentioned once again that the crystal chemistry of mercury in its simple binary oxides is also relevant to the more complicated ternary and quaternary oxides.

6. Comments

All calculations were performed using IBM RS/6000 at the Institute of Inorganic Chemistry of Kiel University. The figures were prepared using a modified ORTEP [56,57] program.

Acknowledgements

The author wishes to thank the Deutsche Forschungsgemeinschaft and the Fonds der Chemischen Industrie for supporting this research by the provision of valuable equipment and financial aid. Thanks are also due to Professor Dr. F. Franzen for editing the manuscript.

References

[1] Hk. Müller-Buschbaum, *Angew. Chem., 89* (1977) 704.
[2] Hk. Müller-Buschbaum, *Angew. Chem., 103* (1991) 741.
[3] H. Rau and A. Rabenau, *Mater. Res. Bull., 2* (1967) 609
[4] E. Kuss, Erzeugung hoher und höchster Drucke im Laboratorium, in W. Foerst and H. Buchholz-Meisenheimer (eds.), *Ullmanns Encyklopädie der Technischen Chemie*, Vol. 2/1, Urban & Schwarzenberger, München, Berlin, 1961, p. 974.
[5] C.J.M. Rooymans, High-pressure technique in preparative chemistry, in P. Hagenmuller (ed.), *Preparative Methods in Solid State Chemistry*, Academic Press, New York, London, 1972.
[6] Hk. Müller-Buschbaum and H. Pausch, *Z. Naturforschung., Teil B, 34* (1979) 371.
[7] Hk. Müller-Buschbaum and H. Pausch, *Z. Naturforschung., Teil B, 34* (1979) 375.
[8] H.-L. Keller, *Dissertation*, University of Giessen, 1973.
[9] H.-L. Keller and Hk. Müller-Buschbaum, *Z. Anorg. Allg. Chem., 393* (1972) 266.
[10] H.-L. Keller and Hk. Müller-Buschbaum, *Z. Naturforschung., Teil B, 28* (1973) 263.

[11] Gmelin, *Volume Oxygen*, System No. 3, Issue No. 8, Verlag Chemie, Weinheim, 1958.
[12] E.C.C. Baly and F.G. Donnan, *J. Chem. Soc. (London), 81* (1902) 907.
[13] J.K.H. Inglis and J.E. Coates, *J. Chem. Soc. (London), 89* (1906) 886.
[14] F.E.E. Germann, *Phys. Z., 14* (1913) 857.
[15] E.H. Amagat, *C.R. Acad. Sci., 100* (1885) 633.
[16] E.H. Amagat, *Ann. Chim. Phys., 29* (1893) 505.
[17] E. Kanda, *Bull. Chem. Soc. Jpn., 12* (1937) 469.
[18] S.N. Putilin, I. Bryntse and E.V. Antipov, *Mater. Res. Bull., 26* (1991) 1299.
[19] S.N. Putilin, E.V. Antipov, O. Chmaissem and M. Marezio, *Nature, 362* (1993) 226.
[20] O. Chmaissem, Q. Huang, S.N. Putilin, M. Marezio and A. Santoro, *Physica C, 212* (1993) 259.
[21] S.M. Loureiro, E.V. Antipov, J.L. Tholence, J.J. Capponi, O. Chmaissem, Q. Huang and M. Marezio, *Physica C, 217* (1993) 253.
[22] E.V. Antipov, J.J. Capponi, C. Chaillout, O. Chmaissem, S.M. Loureiro, M. Marezio, S.N. Putilin, A. Santoro and J.L. Tholence, *Physica C, 218* (1993) 348.
[23] E.V. Antipov, S.M. Loureiro, C. Chaillout, J.J. Capponi, B. Bordet, J.L. Tholence, S.N. Putilin and M. Marezio, *Physica C, 215* (1993) 1.
[24] O. Chmaissem, Q. Huang, E.V. Antipov, S.N. Putilin, M. Marezio, S.M. Loureiro, J.J. Capponi, J.L. Tholence and A. Santoro, *Physica C, 217* (1993) 265.
[25] M. Nunez-Regueiro, J.L. Tholence, E.V. Antipov, J.J. Capponi and M. Marezio, *Science, 262* (1993) 97.
[26] G. Van Tendeloo, C. Chaillout, J.J. Capponi, M. Marezio and E.V. Antipov, *Physica C, 223* (1994) 219.
[27] E.V. Antipov, S.N. Putilin, E.M. Kopnin, J.J. Capponi, C. Chaillout, S.M. Loureiro, M. Marezio and A. Santoro, *Proc. M2HTSC IV, Grenoble, 5–9 July, 1994.*
[28] R. Hoppe and H.J. Röhrborn, *Z. Anorg. Allg. Chem., 329* (1964) 110.
[29] H.D. Wasel-Nielen, *Dissertation*, University of Giessen, 1969.
[30] M. Soll and Hk. Müller-Buschbaum, *J. Less-Common Met., 162* (1990) 169.
[31] M. Soll and Hk. Müller-Buschbaum, *Monatsh. Chem., 121* (1990) 787.
[32] S.N. Putilin, M.G. Rozova, D. Kashporov, E.V. Antipov and L.M. Kovba, *Russ. J. Inorg. Chem., 36* (1991) 928.
[33] M. Soll and Hk. Müller-Buschbaum, *J. Less-Common Met., 175* (1991) 295.
[34] Y.D. Kondrashev, *Kristallografiya, 3* (1958) 696.
[35] S.N. Putilin, S.M. Karzakov and M. Marezio, *J. Solid State Chem., 109* (1994) 406.
[36] Th. Hansen and Hk. Müller-Buschbaum, *Z. Anorg. Allg. Chem., 620* (1994) 1137.
[37] S.N. Putilin, I. Bryntse and M.G. Rozova, *J. Solid State Chem., 93* (1991) 236.
[38] M. Soll and Hk. Müller-Buschbaum, *J. Less-Common Met., 170* (1991) 321.
[39] Chr. L. Teske and Hk. Müller-Buschbaum, *Z. Anorg. Allg. Chem., 371* (1969) 325.
[40] M. Soll and Hk. Müller-Buschbaum, *Monatsh. Chem., 122* (1991) 920.
[41] Th. Hansen and Hk. Müller-Buschbaum, *Z. Anorg. Allg. Chem., 620* (1994) 1471.
[42] U. Treiber, S. Kemmler-Sack and A. Ehmann, *Z. Anorg. Allg. Chem., 487* (1982) 189.
[43] J. Darriet, M. Dirllon, G. Villeneuve and P. Hagenmüller, *J. Solid State Chem., 19* (1976) 213.
[44] J. Wilkens and Hk. Müller-Buschbaum, *J. Alloys Comp., 177* (1991) L31.
[45] J. Wilkens and Hk. Müller-Buschbaum, *J. Alloys Comp., 619* (1993) 517.
[46] H.W. Zandbergen and D.J.W. Ijdo, *Acta Crystallogr., Sect. C, 39* (1983) 829.
[47] Th. Hansen, Hk. Müller-Buschbaum and L. Walz, *Z. Naturforsch., B 50* (1995) 47.
[48] K. Aurivillius, *Acta Crystallogr., 9* (1956) 277.
[49] K. Aurivillius, *Acta Crystallogr., 9* (1956) 685.
[50] K. Aurivillius, *Acta Chem. Scand., 10* (1956) 852.
[51] K. Aurivillius, *Acta Chem. Scand., 18* (1964) 1305.
[52] K. Aurivillius and I.B. Carlsson, *Acta Chem. Scand., 11* (1957) 1069.
[53] K. Aurivillius and I.B. Carlsson, *Acta Chem. Scand., 12* (1958) 1297.
[54] A.W. Sleight, *Inorg. Chem., 7* (1968) 1704.
[55] J. Angenault and A. Rimsky, *C. R. Acad. Sci. Paris, 2266* (1966) 978.
[56] C.K. Johnson, *Rep. ORNL-3794*, Oak Ridge National Laboratory, Oak Ridge, TN, 1965.
[57] K.B. Plötz, *Dissertation*, University of Kiel, 1982.